Dielectric properties of 2-methylbenzimidazolium perchlorate films $C_8H_8N_2-HClO_4$ in the crystalline, liquid crystalline, and ionic liquid phases

© E.V. Balashova, B.B. Krichevtsov

Ioffe Institute, St. Petersburg, Russia
E-mail: balashova@mail.ioffe.ru

Received May 1, 2025
Revised August 8, 2025
Accepted August 11, 2025

Films of 2-methylbenzimidazolium perchlorate (MBI·$HClO_4$) were grown on sapphire Al_2O_3 (0001) substrates. The frequency dependences of the capacitance and $\mathrm{tg}\,\delta$ were studied in the obtained structures under a constant electric field. The studies were carried out in the crystalline phase, the ionic liquid crystal phase, and the ionic liquid phase of MBI·$HClO_4$. In the ionic liquid and ionic liquid crystal phases, a strong effect of the electric field on the dielectric properties and conductivity was found, associated with a change in the parameters of double electric layers arising in the contact region with the electrode. The results of a study of the dielectric properties and conductivity of the structures using dielectric and impedance spectroscopy are presented

Keywords: ionic liquid, ionic liquid crystal, dielectric properties, double electric layers, impedance spectroscopy.

DOI: 10.61011/TPL.2025.12.62793.7981

The dielectric properties of ionic liquids (ILs) and ionic liquid crystals (ILCs) attract much attention at present, since they find application in the production of supercapacitors, batteries, solar cells, and ionogels [1–6]. Supercapacitors may reach high capacitance levels due, in particular, to the formation of electric double layers (EDLs) in the region of the electrode–IL or electrode–ILC contact [4–6]. The properties of ILs, ILCs, and EDLs are normally studied using dielectric or impedance spectroscopy, which makes it possible to identify the mechanisms of conductivity and dielectric response and determine the parameters of the corresponding equivalent electric circuits [7–9].

One important EDL characteristic is the dependence of its parameters on external electric field E_{bias}. This dependence is used, among other things, to produce liquids with an electrorheological effect (i.e., with their viscosity changing reversibly under the influence of an electric field [1]). Such liquids are prepared from ionogels (nanostructures filled with ILs or ILCs).

A relatively small number of papers focused on the influence of an electric field on the dielectric parameters of structures based on pure ILs or ILCs has been published to date. The aim of the present study is to examine the influence of an electric field on the dielectric parameters of 2-methylbenzimidazolium perchlorate $C_8H_8N_2-HClO_4$ (MBI·$HClO_4$) films grown on Al_2O_3 (0001) substrates within the temperature ranges corresponding to IL or ILC phases.

We have recently grown MBI·$HClO_4$ single crystals [10] using the method of slow evaporation from aqueous solutions. It was revealed in room-temperature X-ray diffraction experiments that they are ionic crystals (ICs) formed by ClO_4^- anions and protonated MBI molecules (MBI-H^+) acting as cations. As the temperature increases, the crystal first passes into an intermediate phase and then (at $T_{melt} \approx 440$ K) into a liquid phase. The low-frequency conductivity in the liquid phase is seven orders of magnitude greater than in the IC phase, which is typical of ILs [1–3]. As was demonstrated by polarization-optical studies of MBI·$HClO_4$ films, properties characteristic of the liquid crystal state are observed in the intermediate phase, suggesting that the ILC state is established in this phase [11]. Temperature variations of the dielectric parameters of MBI·$HClO_4$ films grown on different substrates are similar to those observed in single crystals, but the temperatures of IC↔ILC and ILC↔IL transitions in them are somewhat lower [11]. Thus, previous studies have demonstrated that the analysis of temperature behavior of MBI·$HClO_4$ crystals and films provides an opportunity to compare the dielectric properties of the material formed by ClO_4^- and MBI-H^+ ions in different phases: a dielectric ionic crystal, an ionic liquid crystal, and an ionic liquid.

MBI·$HClO_4$ films were grown by evaporation on Al_2O_3 substrates with gold interdigital electrodes (IDEs) pre-deposited onto them. The thickness of these electrodes and the distance between them were 50 μm; the number of pairs was $N = 30$. Following crystallization, large flat MBI·$HClO_4$ crystallites with crystallographic planes ($h0h$) parallel to the film surface were formed on the substrate [11]. These crystallites formed a continuous layer with thickness $h \sim 10\,\mu$m. When the temperature rose above $T \approx 400$ K, the film broke up into individual droplets; in the region of $T \approx 420$ K, droplets become optically isotropic and the IL phase was established. As the temperature decreased, the film passed into the ILC state at $T \approx 410$ K and crystallized (i.e., the IC phase was established) at $T \approx 370$ K.

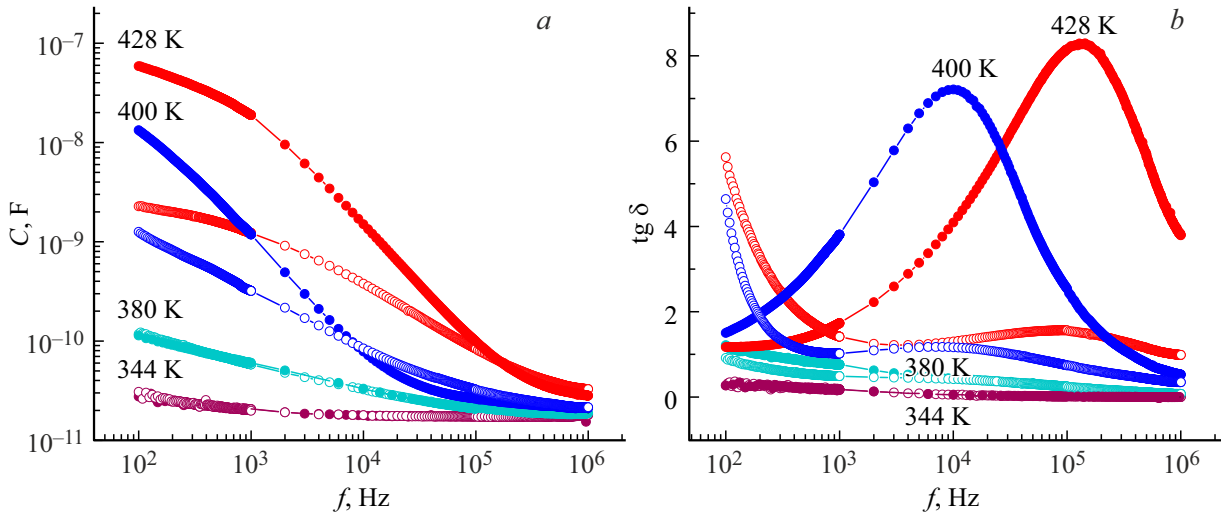

Figure 1. Frequency dependences of capacitance C (a) and $\mathrm{tg}\,\delta$ (b) measured with the temperature increasing for $T = 344$ and 380 K (IC phase), and with the temperature decreasing from the melt at $T = 428$ K (IL phase) to $T = 400$ K (ILC). Filled and open symbols correspond to $U_{bias} = 0$ and $U_{bias} = 3$ V, respectively. Lines are drawn for visual convenience.

Capacitance C and dielectric loss tangent $\mathrm{tg}\,\delta$ of the obtained structures were measured using MIT 9216A and E7-20 *LCR* meters. The IDE system served as electrodes. A direct electric voltage up to $U_{bias}^{\max} = 4$ V ($E_{bias}^{\max} = 0.08$ V/μm) in magnitude was also applied to them. The amplitude of measuring alternating voltage was $U_{dr} = 0.1$ V. Measurements were carried out at frequencies $f = 25-10^6$ Hz and temperatures $T = 295-460$ K. The values of conductivity G, imaginary and real parts of impedance Z' and Z'', and dielectric parameters were determined from the frequency dependences of C and $\mathrm{tg}\,\delta$ and analyzed using the impedance and dielectric spectroscopy methods [7–9]. It should be noted that the diameters of droplets formed in the process of heating were larger than the interelectrode distance (50 μm) and the coupling between the IDE and the film did not vanish when they appeared. This is evidenced, in particular, by a profound increase in capacitance accompanying the formation of droplets caused by a change in the phase state of the material. However, droplets alter the geometry of the structure, which may lead to a certain reduction in capacitance. It was revealed by imaging films with a polarizing microscope that the shape of droplets does not change at a constant temperature and, consequently, does not affect the frequency dependences of capacitance C, $\mathrm{tg}\,\delta$, and conductivity G.

Figure 1 presents the frequency dependences of capacitance C and $\mathrm{tg}\,\delta$ at $U_{bias} = 0$ and 3 V for the IC ($T = 344$ and 380 K), ILC ($T = 400$ K under cooling), and IL ($T = 428$ K) phases. In the IC phase, the capacitance of the structure is low ($C \sim 20-50$ pF) and does not depend on the bias field. Its magnitude is specified primarily by the IDE capacitance. The low-frequency capacitance increases sharply at temperatures above $T \approx 400$ K, which is associated with the emergence of the ILC phase (and the IL phase at $T > 420$ K). The capacitance at $T = 428$ K, $f = 100$ Hz, and $U_{bias} = 0$ is as high as $C \approx 10$ nF, but decreases by almost an order of magnitude to $C \approx 2$ nF at $U_{bias} = 3$ V. As the temperature decreases, similar behavior is observed in the ILC phase. At high frequencies $f \approx 1$ MHz, the structure capacitance does not exceed ~ 50 pF throughout the entire studied temperature range.

A pronounced $\mathrm{tg}\,\delta$ peak is seen at a frequency of approximately 100 kHz in the IL phase in zero DC field. As the temperature decreases in the ILC phase, this peak shifts toward lower frequencies. The application of bias voltage $U = 3$ V results in its partial suppression (Fig. 1, b). In the process of cooling in zero field, the peak in the frequency dependences of $\mathrm{tg}\,\delta$ is observed down to temperature $T \approx 370$ K. The frequency behavior of $\mathrm{tg}\,\delta$ at lower temperatures corresponds to the initial IC state ($\mathrm{tg}\,\delta < 0.1$).

The frequency dispersion of conductivity $G = \omega C\,\mathrm{tg}\,\delta$ and its dependence on bias field U_{bias} are seen in the IL and ILC phases (Fig. 2, a). At frequency $f = 100$ Hz and $T = 428$ K in the IL phase, the conductivity is approximately four orders of magnitude higher than that in the IC phase at $T = 344$ K. The conductivity remains virtually independent of frequency within the $f = 10^3-10^6$ Hz frequency range in both the IL and the ILC phases in zero DC field ($U_{bias} = 0$). This indicates that the contribution of DC conductivity G_{DC} is dominant. At low frequencies $f < 10^3$ Hz, the conductivity decreases due to the EDL formation. The application of bias voltage $U_{bias} = 3$ V results in an approximately order-of-magnitude reduction in conductivity at low frequencies and the emergence of a frequency dependence of conductivity, which is indicative of a significant reduction in G_{DC} within almost the entire frequency range.

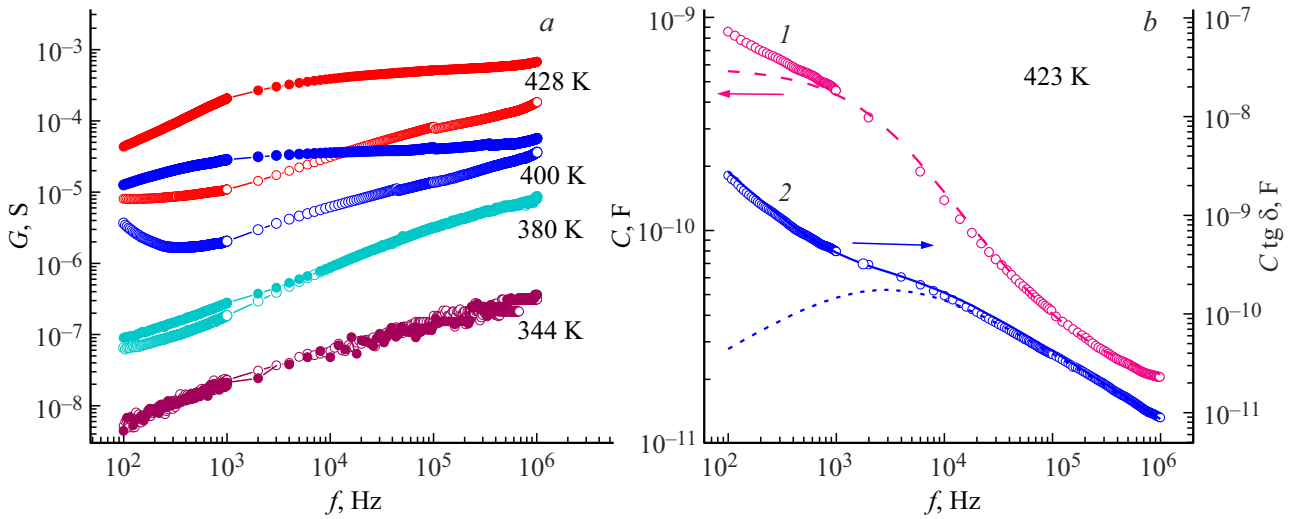

Figure 2. *a* — Frequency dependences of conductivity G in the IC phase ($T = 344$, 380 K under heating), the IL phase ($T = 428$ K), and the ILC phase ($T = 400$ K under cooling from melt) at $U_{bias} = 0$ (filled circles) and $U_{bias} = 3$ V (open circles). Lines are drawn for visual convenience. *b* — Frequency dependences of capacitance C (*1*) and product $C\,\mathrm{tg}\,\delta$ (*2*) in the IL phase at $U_{bias} = 4$ V and $T = 423$ K. Lines represent the calculation results: the solid line corresponds to formula (1), while dashed lines were plotted using formula (1) with the contribution of conductivity neglected.

The large magnitude and strong frequency dependence of capacitance at temperatures corresponding to the IL phase ($T > 420$ K under heating) are indicative of formation of EDLs [12] in the system that are associated with an increase in concentration of anions at the interface at the positive electrode and cations at the negative one. Since the prerequisite for the formation of such layers is displacement of ions, which depends on their mobility and the alternating field applied to the system and takes up a certain amount of time, the capacitance of the structure is characterized by strong frequency dispersion. Note that such frequency dispersion is also observed at temperatures corresponding to the ILC phase (410–370 K after cooling from the melt); the only difference is that the capacitance in this phase is approximately an order of magnitude smaller ($C \sim 1$ nF) than in the IL phase ($C \approx 10$ nF).

The dielectric properties of systems containing double electric layers were analyzed using the dielectric and impedance spectroscopy methods [7–9]. The application of a DC field reduces the conductivity significantly (Fig. 2, *a*), enhancing the relative contribution of relaxation processes to the dielectric parameters and providing an opportunity to characterize the frequency dependences of C and $C^*\,\mathrm{tg}\,\delta$ in the IL phase by the well-known expression for dielectric relaxation of the Cole–Cole type [9] with account for conductivity for complex capacitance $C^* = S(\varepsilon' + i\varepsilon'')$ (S is the geometric factor and ε' and ε'' are the real and imaginary parts of permittivity):

$$C^* = C_\infty + \Delta C/\left(1 + (i\omega\tau)^{1-\alpha}\right) + G_{\mathrm{DC}}/i\omega,$$
$$\mathrm{Re}C^* = C, \qquad \mathrm{tg}\,\delta = \mathrm{Im}C^*/\,\mathrm{Re}C^*, \qquad (1)$$

where $\omega = 2\pi f$ is the angular frequency, C_∞ is the high-frequency background capacitance, ΔC is the difference between the capacitance values at frequencies above and below the relaxation frequency, τ is the average relaxation time, G_{DC} is the DC conductivity, and α is the parameter that leads to symmetrical broadening of $C\,\mathrm{tg}\,\delta$ peaks in comparison with the Debye model, where $\alpha = 0$. The second term on the right-hand side of the first expression in (1) characterizes the Cole–Cole dielectric relaxation, while the third term is the contribution of DC conductivity [9]. Figure 2, *b* presents the experimental and calculated (using expression (1)) frequency dependences of C and $C\,\mathrm{tg}\,\delta$ at $T = 423$ K. A close agreement between the experimental and calculated dependences was obtained with the following parameter values: $C_\infty = 1.65 \cdot 10^{-11}$ F, $\Delta C = 5.7 \cdot 10^{-10}$ F, $\tau = 5.5 \cdot 10^{-5}$ s, $\alpha = 0.3$, $G_{\mathrm{DC}} = 1.65 \cdot 10^{-6}$ S. The high value of parameter α is indicative of a wide distribution of relaxation times and, accordingly, energy barriers in the IL phase. Quantity $\tau = 5.5 \cdot 10^{-5}$ s ($f \sim 3$ kHz) characterizes dielectric relaxation in the IL.

Impedance spectroscopy was used to analyze the charge dynamics in the IL and ILC phases [7,8]. Figure 3 shows the Nyquist diagrams (dependences $Z''(Z')$) in the IL phase at $T = 423$ K and after cooling at $T = 380$ K (ILC phase) and different values of the bias voltage. Calculations were carried out for the equivalent circuit shown in the inset in Fig. 3, *a*, which includes the IDE–film contact resistance (R_s), the IL bulk resistance (R_1), the cell capacitance at high frequency (C_1), and the bounded constant phase (BCP) element, which models the low-frequency impedance of the linear diffusion process in a homogeneous layer of finite thickness [7]. The BCP element impedance is written as $Z_{\mathrm{BCP}}(j\omega) = A^{-1}(j\omega)^{-n}\mathrm{th}[R_0A(j\omega)^n]$ and matches the one of the bounded Warburg (BW) element at $n = 0.5$ [7]. At high frequencies and weak fields, a semicircle character-

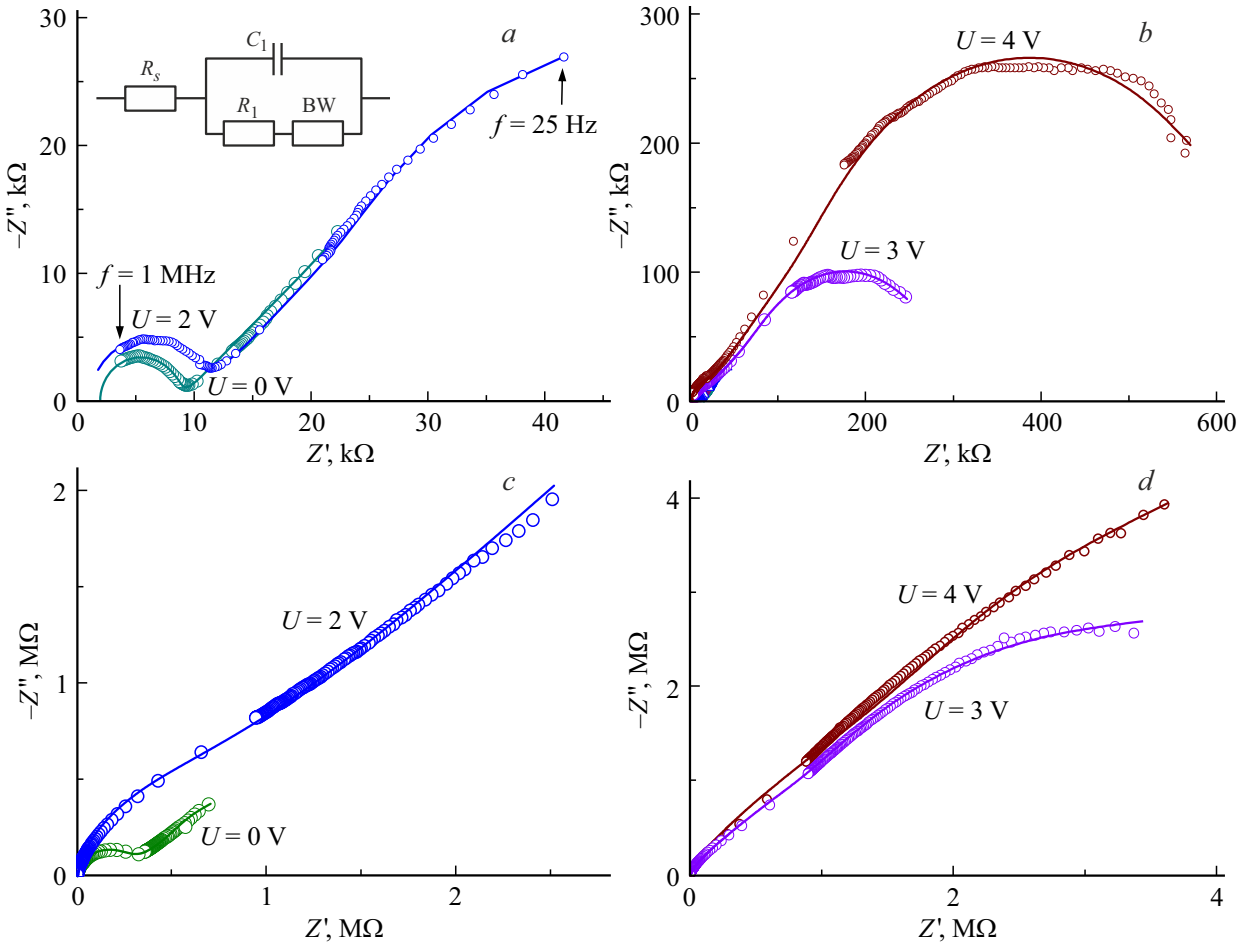

Figure 3. Dependences of imaginary part of impedance Z'' on its real part Z' at $T = 423$ K (IL) for $U_{bias} = 0$ and 2 V (a, c) and $T = 380$ K (ILC) for $U_{bias} = 3$ and 4 V (b, d). Lines represent the results of calculations performed using the equivalent circuit shown in the inset.

izing the relaxation of free charge carriers is seen. The maxima from condition $\omega\tau = 1$ allow one to determine the charge relaxation frequencies: $f = 664$ kHz ($U_{bias} = 0$) and $f = 508$ kHz ($U_{bias} = 2$ V) in the IL phase. These frequencies are dictated by the Maxwellian relaxation of free carriers.

It can be seen from Figs. 1 and 2 that the values of C, $\mathrm{tg}\,\delta$ and conductivity G in the IL and ILC phases depend significantly on both temperature and the applied field, which is reflected in the Nyquist diagrams for different bias voltages presented in Fig. 3. Calculations have demonstrated that the differences between the IL and ILC phases are manifested primarily in parameters A, R_0, which are included in the BCP element, and resistance R_1 (see the table), while the values of C_1, n, and R_s change only slightly. In the IL phase, $C_1 \sim 45$ pF; in the ILC phase, ~ 50 pF. At $U_{bias} = 0$, the value of R_1 in the IL phase is significantly lower than in the ILC. In contrast, parameter A has a greater value in the IL phase. The behavior of parameter R_1 in these phases depends on the bias field. Resistance R_1 increases with the field in the IL phase and in the ILC phase.

Since $n \approx 0.5$ in both phases, product $R_0 A = \delta / D^{0.5}$, where δ is the thickness of the layer in which diffusion proceeds and D is the diffusion coefficient. If we assume that thickness δ is determined by the distance between the IDEs, the relation between the diffusion coefficients in the IL and ILC may be estimated. Although parameters R_0 and A differ greatly, the diffusion coefficients in the IL (D_{IL}) and ILC (D_{ILC}) are of the same order of magnitude at $U_{bias} = 0$. However, when field $U_{bias} = 4$ V is applied, D_{ILC} varies little, while D_{IL} increases by an order of magnitude.

Thus, the study of MBI·$HClO_4$/IDE/Al_2O_3 structures revealed that the frequency dependences of capacitance C and $\mathrm{tg}\,\delta$ in the IL and ILC phases depend significantly on the DC voltage applied to the IDE system. The frequency behavior of imaginary and real parts of permittivity was characterized within the Cole–Cole relaxation model with the contribution of conductivity taken into account. The high value of parameter α indicates that bound charges in the IL move in a complex energy relief characterized by a wide distribution of energy barriers. The characteristic relaxation frequency is $f \approx 3$ kHz.

Parameters A, R_0 characterizing the BCP element and bulk resistance of the structure in the ILC and IL phases R_1

U_{bias}, V	ILC ($T = 380$ K)			IL ($T = 423$ K)		
	A, 10^{-8} $s^{0.5} \cdot \Omega^{-1}$	R_0, MΩ	R_1, kΩ	A, 10^{-8} $s^{0.5} \cdot \Omega^{-1}$	R_0, MΩ	R_1, kΩ
0	9.7	1.12	270	240	0.07	6.7
1	2.5	3.2	275	280	0.07	5.6
2	1.7	20	700	110	0.067	9.3
3	1.0	62.5	530	21	0.28	15
4	0.8	10.5	570	6.5	0.64	16

The dynamics of free carriers in the IL and ILC phases was characterized using an equivalent circuit with a bounded Warburg element. These phases have significantly different parameters A and R_0 of the BCP element, which characterizes linear diffusion processes in a homogeneous layer of finite thickness. The application of an electric field in the ILC and IL phases has different effects on these parameters and on diffusion coefficient D. The Maxwell relaxation frequency in the IL phase decreases from $f = 664$ to 508 kHz when voltage $U = 2$ V is applied.

In future studies, we plan to fabricate and examine structures in the form of planar capacitors with MBI·$HClO_4$ layers embedded in the interelectrode space in the region of the ILC and IL phases.

Conflict of interest

The authors declare that they have no conflict of interest.

References

[1] D. MacFarlane, N. Tachikawa, M. Forsyth, J. Pringle, P. Howlett, G. Elliott, J. Davis, Jr., M. Watanabe, P. Simon, C. Austen Angell, Energy Environ. Sci., **7**, 232 (2014). DOI: 10.1039/C3EE42099J

[2] T. Zhou, Ch. Guid, L. Sun, Y. Hua, H. Lyu, Z. Wange, Zh. Song, G. Yu., Energy. Chem. Rev., **123** (21), 12170 (2023). DOI: 10.1021/acs.chemrev.3c00391

[3] *Dielectric properties of ionic liquids*, ed. by M. Paluch (Springer International Publ., Switzerland, 2016). DOI: 10.1007/978-3-319-32489-0

[4] K. Binnemans, Chem. Rev., **105**, 4148 (2005). DOI: 10.1021/cr0400919

[5] A.F.M. Santos, J.L. Figueirinhas, M. Dionísio, M.H. Godinho, L.C. Branco, Materials, **17**, 4563 (2024). DOI: 10.3390/ma17184563

[6] Q. Ruan, M. Yao, D. Yuan, H. Dong, J. Liu, X. Yuan, W. Fang, G. Zhao, H. Zhang, Nano Energy, **16** (2), 108087 (2023). DOI: 10.1016/j.nanoen.2022.108087

[7] *Impedansnaya spektroskopiya: teoriya i primenenie*, Ed. by E.S. Buyanova (Izd. Ural. Univ., Ekaterinburg, 2017) (in Russian). http://elar.urfu.ru/handle/10995/52395

[8] S. Wang, J. Zhang, O. Gharbi, V. Vivitr, M. Gao, M.E. Orazem, Nat. Rev. Meth. Primers, **1**, 41 (2021). DOI: 10.1038/s43586-021-00039-w

[9] *Broadband dielectric spectroscopy*, ed. by F. Kremer, A. Schönhals (Springer-Verlag, Berlin–Heidelberg, 2003). DOI: 10.1007/978-3-642-56120-7

[10] E. Balashova, A. Zolotarev, A.A. Levin, V. Davydov, S. Pavlov, A. Smirnov, A. Starukhin, B. Krichevtsov, H. Zhang, F. Li, H. Luo, H. Ke, Materials, **16**, 1994 (2023). DOI: 10.3390/ma16051994

[11] E.V. Balashova, A.A. Levin, B.B. Krichevtsov, Tech. Phys. Lett., **50** (12), 157 (2024). DOI: 10.61011/PJTF.2024.24.59447.6466k.

[12] S. Shiraishi, in *Carbon alloys*, ed. by E. Yasuda, M. Inagaki, K. Kaneco, M. Endo, A. Oya, Y. Tanabe (Elsevier Science, 2003), ch. 27, p. 447–457. DOI: 10.1016/B978-008044163-4/50027-9

Translated by D.Safin